

UCSF

UC San Francisco Previously Published Works

Title

Early animal model evaluation of an implantable contrast agent to enhance magnetic resonance imaging of arterial bypass vein grafts

Permalink

<https://escholarship.org/uc/item/0sv321pc>

Journal

Acta Radiologica, 59(9)

ISSN

0284-1851

Authors

Mitsouras, Dimitrios
Tao, Ming
de Vries, Margreet R
[et al.](#)

Publication Date

2018-09-01

DOI

10.1177/0284185117753656

Peer reviewed



Published in final edited form as:

Acta Radiol. 2018 September ; 59(9): 1074–1081. doi:10.1177/0284185117753656.

Early Animal Model Evaluation of an Implantable Contrast Agent to Enhance Magnetic Resonance Imaging of Arterial Bypass Vein Grafts

Dimitrios Mitsouras, PhD¹, Ming Tao, MD², Margreet de Vries, PhD³, Kaspar Trocha, MD², Oscar R. Miranda, PhD^{4,5}, Praveen Kumar Vemula, PhD^{4,5}, Kui Ding², Amir Imanzadeh¹, Frederick J. Schoen, MD PhD⁶, Jeffrey M. Karp, PhD^{4,5}, C. Keith Ozaki, MD², Frank J. Rybicki, MD PhD^{1,7}

¹Applied Imaging Science Laboratory, Department of Radiology, Brigham and Women's Hospital, Boston, MA, USA ²Department of Surgery, Brigham and Women's Hospital, Boston, MA, USA.

³Department of Surgery, Einthoven Laboratory for Experimental Vascular Medicine, Leiden University Medical Center, Leiden, The Netherlands ⁴Harvard Stem Cell Institute, Harvard University, Boston, Massachusetts, USA. ⁵Harvard-MIT Division of Health Science and Technology, Department of Medicine, Brigham and Women's Hospital, Boston, Massachusetts, USA. ⁶Department of Pathology, Brigham and Women's Hospital, Boston, MA, USA ⁷Ottawa Hospital Research Institute and Division of Medical Imaging, The Ottawa Hospital Department of Radiology, University of Ottawa, Ottawa, ON, Canada

Abstract

Background: Noninvasive monitoring of autologous vein graft (VG) bypass grafts is largely limited to detecting late luminal narrowing. Although magnetic resonance imaging (MRI) delineates vein graft intima, media and adventitia, which may detect early failure, the scan time required to achieve sufficient resolution is at present impractical.

Purpose: To study VG visualization enhancement *in vivo* and delineate whether a covalently attached MRI contrast agent would enable quicker longitudinal imaging of the VG wall.

Material and Methods: Sixteen 12 week-old male C57BL/6J mice underwent carotid interposition vein grafting. The inferior vena cava (IVC) of 9 donor mice was treated with a Gadolinium-diethylenetriaminepentaacetic acid (Gd-DTPA) based contrast agent, with control VGs labeled with a vehicle. T1-weighted MRI was performed serially at 1, 4, 12, and 20 weeks post operatively. A portion of animals was sacrificed for histopathology following each imaging time point.

Results: MRI signal-to-noise (SNR) and contrast-to-noise ratios (CNR) were significantly higher for treated VGs in the first 3 time points (1.73x higher signal-to-noise ratio, $p=0.0006$, and 5.83x higher contrast-to-noise ratio at the first time point, $p=0.0006$). However, the MRI signal

Address Correspondence to: Frank J. Rybicki MD PhD, Chair and Chief, Department of Radiology, The University of Ottawa, ON, Canada. frybicki@toh.ca.

Conflicts of Interest: None.

enhancement decreased consistently in the study period, to 1.29x higher SNR and 2.64x higher CNR, by the final time point. There were no apparent differences in graft morphometric analyses in Masson's trichrome-stained cross-sections, including ideal lumen area.

Conclusion: A MRI contrast agent that binds covalently to the VG wall provides significant increase in T1-weighted MRI signal with no observed adverse effects in a mouse model. Further optimization of the contrast agent to enhance its durability is required.

Keywords

Magnetic resonance imaging; gadolinium contrast agent; vein graft; contrast enhanced imaging; targeted contrast agent

Introduction

Autologous vein graft (VG) arterial bypass is an evidence-based treatment for selected patients with infra-inguinal lower extremity or coronary occlusive disease. Almost 40% of lower extremity VGs develop occlusive lesions or fail within a year¹, and nearly half of cardiac VG patients will develop a graft problem (75% stenosis) within a year². Numerous studies support a role for enhanced VG surveillance³⁻⁶. At present, noninvasive duplex screening is limited to detecting late luminal narrowing secondary to intimal hyperplasia (IH), which has been viewed as the primary etiology of early graft failure as well as data supporting an important role for negative wall remodeling^{7, 8} and adventitial processes in vascular lesions⁹⁻¹². Decades of VG research focusing on IH have failed to produce effective preventative or therapeutic strategies^{1, 2, 10, 13-20}. More recent efforts using mathematical models combined with patient specific flow dynamics have provided further insight into the complex process of VG failure²¹. Nevertheless, given the persisting morbidity and mortality associated with VG failure, enhanced surveillance approaches are needed.

Magnetic resonance imaging (MRI) can delineate the human VG wall (Fig. 1) and differentiate the media and neo-intima from the adventitia^{22, 23}. However, using available magnetic field strengths and scan times, where 10 minutes allows for only 3.6cm coverage, craniocaudal coverage is limited in order to achieve the high resolution and signal-to-noise ratio (SNR) required to image the VG. This limitation persists even with the use of reduced field-of-view and high sampling efficiency MRI sequences²³⁻²⁵. Thus while MRI may be potentially useful for characterizing focal lesions *in vivo* over time²⁵⁻²⁷, it is at present insufficient for surveillance of e.g., a typical 40-80 cm lower extremity VG. Furthermore, the VG wall and adjacent tissues such as muscle, scar tissue, and edema, often have similar relaxation properties, rendering tissue discrimination difficult throughout the VG circumference (Fig. 1).

To address these limitations of VG surveillance, we have previously demonstrated an *ex vivo* MRI signal enhancement of the human vein wall via use MR contrast agents that are immobilized onto the tissue using a covalent amide bond^{28, 29}. The contrast enhancement of the vein wall in that study persisted over a 4-month period, suggesting the opportunity for long-term *in vivo* tissue signal enhancement that could allow longitudinal follow-up by MRI. The purpose of the present proof of approach work was to study VG visualization

enhancement in the intact mammal and to delineate the biologic effects and durability of this implantable contrast agent.

Materials & Methods

Study Design

Animal studies were approved by our Institutional Animal Care and Use Committee for all 32 mice. Sixteen animals were included in the study. In 7 control animals, the VG was treated with a non-Gd containing vehicle. In 9 animals, the VG was covalently labeled with the implantable Gd-DTPA contrast agent. Magnetic resonance imaging of each animal was performed serially at 1, 4, 12, and 20 weeks post implantation. Two controls and two experimental mice were sacrificed for histopathologic studies following imaging at each time point, except for the last time point where only 1 control and 3 contrast-treated animals remained.

Gd-DTPA Modification and Immobilization Chemistry

As previously described²⁸, Gd-DTPA (Diethylenetriaminepentaacetic acid gadolinium³⁺ dihydrogen) complex was modified to react with primary amines (NH₂), such as those found on the surface of cells, to form a covalent amide bond based on *N*-hydroxysuccinamide ester coupling chemistry³⁰. Importantly, this approach does not compromise cell properties such as viability and proliferation³⁰. Briefly, carboxylic acid groups in the Gd-DTPA complex (250 mM, 1 equivalent) were coupled with NHS (2.5 M, 10 equivalents) using *N,N'*-diisopropylcarbodiimide (DIC, 2.5 M, 10 equivalents) as a coupling agent. The total volume for the activation process was fixed on 10 mL (3.8712 mL of DIC into 6.1288 mL of dimethyl sulfoxide [DMSO]). For control vehicle, 20% DMSO solution (2 mL of DMSO, 8 mL water) without contrast agent were used.

Vein Graft Procedure and Venous Segment *ex vivo* Labeling

Sixteen 12 week-old male C57BL/6J mice (Jackson Laboratory, Bar Harbor, ME) were used. Animals were maintained on 12-hour light-dark cycle, and received water and standard chow *ad libitum*. All animal experiments were performed in accordance with guidelines of the Public Health Services, US Department of Agriculture and National Institutes of Health. Controls and experimental animals underwent carotid interposition VGs as previously reported^{31,32}. Briefly, each mouse was placed into an induction chamber with 2% isoflurane. Anesthesia was then maintained with continuous 1.0–1.25% isoflurane inhalation. Surgical procedures were performed aseptically and animal body temperature was maintained at 37°C on a heated water pad. A vertical midline neck incision was performed and right carotid artery was dissected then ligated with 8–0 nylon suture at the midpoint and divided. After clamping, ligatures were removed and the proximal and distal artery ends were everted over polyetheretherketone cuffs (Zeus Inc., Orangeburg, SC).

The thoracic inferior vena cava (IVC) from a separate donor mouse (length ~3–4mm) was dissected from surrounding tissue and flushed with heparinized saline and tied at proximal and distal ends to ensure only the adventitia of the graft would be in contact with the labeling agent. The harvested IVC segment was incubated with MRI contrast agent solution

or control vehicle for 1 minute. Only the outside of the venous conduit was in contact with contrast agent. After incubation, vein was rinsed with saline. Finally the VG segment was positioned over the cuffed arterial ends and secured with sutures, creating a carotid interposition VG. Following surgery, buprenorphine (0.1mg/kg) was administered to relieve pain and mice were observed for 2 hours for signs of hemorrhage and hypothermia post-operatively

At time of harvest mice were anesthetized using isoflurane inhalation 5% induction, 2% maintenance. Blood was collected by percutaneous cardiac puncture and vessels and selected organs were harvested. Cervical dislocation was performed on the anesthetized mouse to ensure death.

Vein Graft Morphology/Histopathology

At 1 week, 4 week, 12 week, and 20 week time points post operatively, VG, liver, and kidney were harvested. The thorax was opened and left ventricle was punctured using 25-gauge needle for perfusion with Lactated Ringer's solution. Blood was drained through an incision in the IVC, then perfusion solution was changed to 10% neutral buffered formalin (4% formaldehyde). VG, liver, and kidney were harvested, fixed and embedded in paraffin. Using the cuff edge as a landmark, cross-sections at 200 μ m, 400 μ m, and 600 μ m distances were collected to represent the VG.

Masson's trichrome stain was used on cross sections to visualize the VG wall. Digitized microscopic images were captured and analyzed using a computerized imaging system (Zeiss Axio A1 microscope, Vision 4.7, Carl Zeiss Inc, Oberkochen, Germany). Morphometric analysis was performed by tracing the endothelial cell lining the length of the internal elastic lamina (IEL), and the length of outer wall/boundary of the adventitia. Intimal thickness, intimal area, media and adventitia thickness, media and adventitia area, lumen area, total wall thickness, total wall area, and ratios among parameters were calculated from the measured circumferences. An ideal lumen area was calculated assuming a disk-shaped structure under *in vivo* conditions. Mouse kidneys and livers were visualized using Masson's trichrome and hematoxylin and eosin stained sections at 3 sagittal locations in each specimen, then evaluated by a blinded pathologist for evidence of toxic effects.

In Vivo MRI Imaging

MR imaging was performed using a small-animal 7 Tesla MRI system (Biospec 70/20, Bruker BioSpin MRI GmbH, Ettlingen, Germany). Each animal was imaged separately at each time point. Localizer scans were first acquired in each of the axial, coronal and sagittal planes using a two-dimensional (2D) rapid acquisition with relaxation enhancement sequence to determine the three-dimensional (3D) orientation of the VG. Sequence parameters were 0.5–0.75 mm slice thickness, 100 \times 100 μ m in-plane resolution, 0.4–1.3 s TR, 8.7 ms TE, 2 signal averages, 192 \times 256 encoding matrix and echo train length of 4. T1-weighted MR images were acquired orthogonal to VG course to produce cross-sectional images of the VG lumen and wall using 2D fast low angle shot sequence. Parameters for this acquisition were 45° flip angle, 0.4 mm slice thickness, 80 \times 80 μ m in-plane resolution, 240 \times 320 encoding matrix, \pm 22 kHz BW, 114 ms TR and 4.2 ms TE.

MR Image Analyses

T1-weighted MR image signal measurements were performed using manually-placed regions-of-interest (ROIs). ROIs were placed in an empty image region, referring to a portion of the image that contains no signal-producing material (i.e., air), in order to assess noise, as well as in VG wall tissue and tissues surrounding the VG (Fig. 2). At least two ROI measurements were averaged for each image for both VG wall tissue and surrounding tissue (Fig. 2). Averaged ROI signal measurements in each individual image were then used to calculate a) the signal-to-noise ratio (SNR) of VG tissue, calculated as the average signal in the VG wall tissue ROIs in that image divided by standard deviation of the signal in a large ROI placed in the portion of the image containing only air, and b) the contrast-to-noise ratio (CNR) of the VG wall tissue compared to its surroundings, calculated as average signal in VG wall tissue ROIs minus the average signal in surrounding tissue ROIs divided by the standard deviation of the signal in a large ROI placed in the portion of the image containing only air. SNR and CNR for each animal at each time point were obtained by averaging individual image SNR and CNR measurements across all images of the animal wherein measurements could be successfully performed.

Statistical Analyses

The animal model and imaging tested is expensive and labor intensive, thus the number of independent observations was relatively small in this proof of approach study. Data with very small numbers of observations are thus presented without error bars. For the limited comparative analyses completed, SNR and CNR parameters derived from the MRI experiments for two time points were compared using unpaired non-parametric Mann-Whitney U-test, except for the last time point as only a single control remained in that time point so a parametric t-test was performed. A *p*-value of 0.05 was considered statistically significant. Gd peak identification in the Energy-dispersive X-ray spectroscopy (EDAX) spectrum was automated as the spectrum was built up during scanning.

Results

Vein Graft Function and Morphology

All animals survived the VG procedure and recovery. Six of the 16 grafts occluded before their harvest time point (2 out of 7 controls, 4 out of 9 treatments, Fisher's exact test $p = 0.63$). Occluded grafts were considered a functional failure and were therefore excluded from VG histological analyses. While detailed analysis may yield further details occluded grafts early occlusion is often secondary to technique and late failure is often secondary to thrombosis. In the remaining animals there were no gross microscopic differences between treated and control VG (Fig. 3), or in calculated ideal lumen area or the ratios of intimal/(medial and adventitial) area measurements (Fig. 4).

Toxicity

There was no clinically apparent effect of the VG treatment on the mouse wound healing and behavior, nor was there microscopic evidence of renal or hepatic toxicity.

MRI

One animal with a labeled VG scheduled for sacrifice at the 3rd time point was excluded from analysis as the VG wall could not be localized at any imaging time point, secondary to early occlusion and/or slow flow. Of the remaining animals, each yielded on average 3 MRI slices at each time point wherein the VG was successfully visualized and measurements performed (Fig. 5).

Both SNR and CNR of the control animal VG wall remained approximately constant throughout the four imaging time points (average SNR across 4 time points=15.6, $p=0.173$; average CNR across four time points=2.41, $p=0.707$, Fig. 6). Although both SNR and CNR were higher for labeled than control VGs at all time points, both decreased over time. SNR of labeled VGs was between 1.73 times to 1.29 times higher than that of controls, and the difference was statistically significant in the first three time points where it could be tested (24.49 vs 16.7, $p=0.0006$; 23.56 vs 15.76, $p=0.0079$; 27.5 vs 16.18, $p=0.02$; and 17.89 vs 13.9; for each time point, respectively). CNR was 5.83 to 2.64 times higher than that of control VGs (Fig. 6) and was also statistically significantly larger than that of controls in the first three time points (11.23 vs 1.95, $p=0.0006$; 11.74 vs 2.75, $p=0.0079$; 8.4 vs 2.05, $p=0.02$; and 6.24 vs 2.36; at each time point, respectively).

Discussion

Despite decades of research, VG failure remains a significant problem³³. Lower extremity graft surveillance using Doppler ultrasonography estimates disease severity by detecting relative increases in flow velocity associated with a stenosis, or overall decrease in graft velocities, often late findings. Coronary bypass grafts are not accessible for duplex surveillance. Because of limited spatial resolution and tissue contrast, there is little further potential information that can be obtained from ultrasound regarding the VG wall and graft remodeling in early disease.

Therefore the diverse soft tissue and flow-sensitive contrast opportunities, non-invasiveness, and use of non-ionizing radiation render MRI ideally suited for frequent long-term follow-up of lower extremity grafts. Multi-contrast MRI in particular has been considered a candidate for imaging of IH and VG wall remodeling^{22, 25}, both of which are implicated in VG failure. There are however two main limitations of MR for VG imaging. The first is limited craniocaudal coverage that is achievable in reasonable scan times²². This limitation may be overcome by the use of volume-selective, high sampling efficiency MRI sequences^{23, 34, 35}. The second limitation stems from similar relaxation properties of adventitial tissue compared to adjacent tissues. Human VG adventitia is characterized by a bi-exponential MR signal decay with T2 times of ~36 (~83%) and 135 ms²², which are similar to those of muscle and subcutaneous fat³⁶. This often renders discrimination of the VG wall difficult throughout its circumference (Fig. 1), and cannot be overcome using endogenous MRI contrast mechanisms.

This study demonstrates for the first time *in vivo* use of an implantable MRI contrast agent to enhance VG wall tissue with the potential to address both these limitations. Using this contrast agent in a murine VG model, we were able to achieve significant increase in VG

wall tissue T1-weighted MR image CNR of 2.6 to 5.8-fold for up to 20 weeks after implantation. To achieve an increase in CNR by a factor of 2, an increase in scan time by a factor of 4 is otherwise required. Thus, this agent can potentially offer significant gains for non-invasive VG wall imaging. Furthermore, the increased CNR offered can be used to either shorten scan time or enhance separation to surrounding tissues. Although the increase in CNR is primarily due to T1 relaxation time shortening of the VG tissue, the Gd-DTPA-based agent also shortens its T2 relaxation time²⁸, which can potentially further aid in the separation of the VG wall from surrounding tissues. Although labeling of the VG with the agent was performed with the IVC ends tied, allowing only the adventitia of the vessel to be in contact with the labeling vehicle, the MRI signal enhancement was observed throughout the layers of the vessel wall (see Fig. 5).

Unlike our prior results in *ex vivo* settings, however²⁸, there was loss of contrast enhancement with time *in vivo* indicating decreased Gd level, and some form of contrast medium possibly de-binding to the vessel wall. Free Gd-molecule leaking from the graft would likely be released as Gd ions rather than a modified DTPA molecule. DTPA does not have any hydrolyzable bonds, and has been immobilized to the tissue through an amide bond formation; therefore, it would be unlikely that DTPA molecule could be detached from the tissue. Segmental degradation of the contrast enhancement was visible by week 12 post-implantation, and potential gains in SNR and CNR were significantly reduced by week 20. Although the loss of contrast is a disadvantage of the current technique, depending on the source it can potentially either be remediated by modification of the contrast agent, or potentially used as a source of information regarding the underlying processes of VG maturation, if indeed it relates to the loss or dilution of cross-linked tissue components.

This study supports that a gadolinium-based contrast agent is amenable to application in the surgical setting with a 1-minute “labeling” reaction time that could enable longitudinal follow-up of VG maturation with MRI. Although our results suggest that safe future human application may one day appear realizable, a current attractive application is toward the study of IH in animal models. Non-invasive *in vivo* imaging with MRI offers one of the few pathways to longitudinally study VG maturation and explore the biological processes leading to VG failure.

Nonetheless, our study is primarily limited by the small number of grafted animals available. Specifically, we were unable to robustly statistically test histomorphometric variables of VGs, as at most two animals in each group were sacrificed at each imaging time point. Also the evaluation of renal and hepatic toxicity was based on histologic features alone. We acknowledge that free gadolinium is highly toxic, and would lead to complications if exposed to tissues thus; specific care is taken in the manufacturing of gadolinium agents where Gd is in a chelated form. Additionally of importance is the risk of renal failure in patients following surgery with concomitant implantation of a Gd-containing graft. This risk of possible nephrogenic systemic fibrosis in patients with pre-existing renal dysfunction (glomerular filtration rate [GFR], less than 30 mL/min/1.73 m²) or acute kidney injury (1) carries an approximate incidence of 2–5%³⁷. Yet a recent prospective cohort study revealed no cases of nephrogenic systemic fibrosis in patients at an increased risk of its development over a two year time period.³⁸ Furthermore, the risk of allergy-like reactions is clinically

relevant however severe reactions are extremely rare (0.04%) and to develop allergy-like reaction, typically Gd concentration should be much higher than the concentrations used for functionalization. Estimating a human weighing 60 kg, the amount of Gd required to label a vein graft (0.89 mg) would be 0.015 mg/kg, which amounts to 0.012–0.025% of the mice LD₅₀. Finally

Future studies, potentially with an improved contrast agent as discussed above, could directly compare MRI versus histology derived measurements of the vessel wall and lumen in larger animal models. Based on our preliminary results, we hypothesize that MRI using the contrast agent may be able to provide luminal and wall measurements, and potentially supplant study designs that rely on animal sacrifice for histology measurements at each time point.

In conclusion a Gd-DTPA-based MRI contrast agent provided a 2.6 to 5-fold increase in *in vivo* T1-weighted MRI contrast-to-noise ratio of the VG wall tissue in a murine model. The enhancement, although significant for up to 12 weeks post VG implantation, decreased consistently in the 20-week study period, indicating that the technique requires improvements in binding efficiency and/or stability of the modified gadolinium chelate.

Acknowledgements

The authors would like to thank Dr. Amir Imanzadeh, MD . and Miss Tehya Johnson for their help in data collection.

Funding Sources: American Heart Association 12GRNT9510001 and 12GRNT1207025; Lea Carpenter du Pont Vascular Surgery Fund; Carl and Ruth Shapiro Family Foundation; NIH NIBIB Grant K01-EB015868.

Biography

All authors listed bellow have contributed significantly to the conception or design of the work; or the acquisition, analysis, or interpretation of data for the manuscript entitled “Early Animal Model Evaluation of an Implantable Contrast Agent to Enhance Magnetic Resonance Imaging of Arterial Bypass Vein Grafts”. Also all authors give approval of the pending version to be published; and all authors agree to be accountable for all aspects of the work.

Dimitrios Mitsouras, PhD. Applied Imaging Science Laboratory, Department of Radiology, Brigham and Women’s Hospital, Boston, MA, USA.

First author who contributed extensively to the study design, development and execution. Dr. Mitsouras was extensively involved in the radiology protocols, image analysis, quantification and writing of manuscript.

Ming Tao, MD. Department of Surgery, Brigham and Women’s Hospital, Boston, MA, USA. Dr. Tao was involved directly with the microsurgery vein graft procedure in mice. She also processed, embedded and cut the vein grafts for histomorphometric analysis. Additionally she contributed greatly to data analysis and completion of manuscript.

Margreet de Vries, PhD. Department of Surgery, Einthoven Laboratory for Experimental Vascular Medicine, Leiden University Medical Center, Leiden, The Netherlands. Dr. de Vries was involved in performing the microsurgical vein graft procedure in concert with Dr. Tao. Due to the precise nature and difficulty of the technique, two experienced microsurgeons aided in execution of the study. She also participated in the manuscript drafting.

Kaspar Trocha, MD. Department of Surgery, Brigham and Women's Hospital, Boston, MA, USA. Department of Surgery, Brigham and Women's Hospital, Boston, MA, USA. Dr. Trocha was primary in the data assimilation, presentation, and all aspects of manuscript preparation and submission.

Oscar R. Miranda, PhD. Harvard Stem Cell Institute, Harvard University, Boston, Massachusetts, USA. Harvard-MIT Division of Health Science and Technology, Department of Medicine, Brigham and Women's Hospital, Boston, Massachusetts, USA. Key contributor for the development of the contrast binding strategies, completion of compound generation, and application to the vein grafts. He also actively participated in manuscript drafting.

Praveen Kumar Vemula, PhD. Harvard Stem Cell Institute, Harvard University, Boston, Massachusetts, USA. Harvard-MIT Division of Health Science and Technology, Department of Medicine, Brigham and Women's Hospital, Boston, Massachusetts, USA. Key contributor for the development of the contrast binding strategies, completion of compound generation, and application to the vein grafts. He also actively participated in manuscript drafting.

Kui Ding. Department of Surgery, Brigham and Women's Hospital, Boston, MA, USA. Spearheaded microscopic analyses and also assisted with the animal models. He also actively participated in manuscript drafting.

Amir Imanzadeh. Applied Imaging Science Laboratory, Department of Radiology, Brigham and Women's Hospital, Boston, MA, USA. Worked largely on the image analyses and interpretations. He also actively participated in manuscript drafting.

Frederick J. Schoen, MD, PhD. Department of Pathology, Brigham and Women's Hospital, Boston, MA, USA. Dr. Schoen was performed histologic examination and interpretation of the renal and hepatic tissue. He also actively participated in manuscript drafting.

Jeffrey M. Karp, PhD. Harvard Stem Cell Institute, Harvard University, Boston, Massachusetts, USA. Harvard-MIT Division of Health Science and Technology, Department of Medicine, Brigham and Women's Hospital, Boston, Massachusetts, USA. Worked to gain funding for the project, and also led development of the contrast binding strategies and compound generation. He also actively participated in manuscript drafting.

C. Keith Ozaki, MD. Department of Surgery, Brigham and Women's Hospital, Boston, MA, USA. Dr. Ozaki led the non-imaging aspects of the project. He was key in gaining funding for the project, and he oversaw the biologic research protocol and organized the necessary collaborations for project completion. He also worked with the co-authors on manuscript preparation and finalization.

Frank J. Rybicki MD, PhD. Ottawa Hospital Research Institute and Division of Medical Imaging, The Ottawa Hospital. Department of Radiology, University of Ottawa, Ottawa, ON, Canada. Senior author that was responsible for overall research design in collaboration with Dr. Karp and Dr. Ozaki. He led gaining funding for the project, and he oversaw the research protocol and worked with the authors on manuscript preparation and finalization.

References

1. Conte MS, Bandyk DF, Clowes AW, et al. Results of PREVENT III: a multicenter, randomized trial of edifoligide for the prevention of vein graft failure in lower extremity bypass surgery. *JVascSurg.* 2006; 43: 742–51.
2. Alexander JH, Hafley G, Harrington RA, et al. Efficacy and safety of edifoligide, an E2F transcription factor decoy, for prevention of vein graft failure following coronary artery bypass graft surgery: PREVENT IV: a randomized controlled trial. *JAMA.* 2005; 294: 2446–54. [PubMed: 16287955]
3. Berceci SA, Hevelone ND, Lipsitz SR, et al. Surgical and endovascular revision of infrainguinal vein bypass grafts: analysis of midterm outcomes from the PREVENT III trial. *Journal of vascular surgery.* 2007; 46: 1173–9. [PubMed: 17950564]
4. Kirby PL, Brady AR, Thompson SG, Torgerson D and Davies AH. The Vein Graft Surveillance Trial: rationale, design and methods. VGST participants. *European journal of vascular and endovascular surgery : the official journal of the European Society for Vascular Surgery.* 1999; 18: 469–74.
5. Baldus S, Koster R, Elsner M, et al. Treatment of aortocoronary vein graft lesions with membrane-covered stents: A multicenter surveillance trial. *Circulation.* 2000; 102: 2024–7. [PubMed: 11044414]
6. Mills JL Sr., Wixon CL, James DC, Devine J, Westerband A and Hughes JD. The natural history of intermediate and critical vein graft stenosis: recommendations for continued surveillance or repair. *Journal of vascular surgery.* 2001; 33: 273–8; discussion 8–80. [PubMed: 11174778]
7. Lau GT, Ridley LJ, Bannon PG, et al. Lumen loss in the first year in saphenous vein grafts is predominantly a result of negative remodeling of the whole vessel rather than a result of changes in wall thickness. *Circulation.* 2006; 114: I435–40. [PubMed: 16820615]
8. Kaneda H, Terashima M, Takahashi T, et al. Mechanisms of lumen narrowing of saphenous vein bypass grafts 12 months after implantation: an intravascular ultrasound study. *Am Heart J.* 2006; 151: 726–9. [PubMed: 16504641]
9. Kalra M and Miller VM. Early remodeling of saphenous vein grafts: proliferation, migration and apoptosis of adventitial and medial cells occur simultaneously with changes in graft diameter and blood flow. *J Vasc Res.* 2000; 37: 576–84. [PubMed: 11146412]
10. Jiang Z, Yu P, Tao M, et al. TGF-beta- and CTGF-mediated fibroblast recruitment influences early outward vein graft remodeling. *Am J Physiol Heart Circ Physiol.* 2007; 293: H482–8. [PubMed: 17369455]
11. Chatterjee TK, Stoll LL, Denning GM, et al. Proinflammatory phenotype of perivascular adipocytes: influence of high-fat feeding. *Circ Res.* 2009; 104: 541–9. [PubMed: 19122178]
12. Robinson ST and Taylor WR. Beyond the adventitia: exploring the outer limits of the blood vessel wall. *Circ Res.* 2009; 104: 416–8. [PubMed: 19246683]
13. Banno H, Takei Y, Muramatsu T, Komori K and Kadomatsu K. Controlled release of small interfering RNA targeting midkine attenuates intimal hyperplasia in vein grafts. *JVascSurg.* 2006; 44: 633–41.
14. Murday AJ, Gershlick AH, Syndercombe-Court YD, et al. Intimal hyperplasia in arterial autogenous vein grafts: a new animal model. *CardiovascRes.* 1983; 17: 446–51.
15. Bassiouny HS, White S, Glagov S, Choi E, Giddens DP and Zarins CK. Anastomotic intimal hyperplasia: mechanical injury or flow induced. *JVascSurg.* 1992; 15: 708–16.
16. Davies MG and Hagen PO. Pathophysiology of vein graft failure: a review. *EurJ Vasc EndovascSurg.* 1995; 9: 7–18.

17. Motwani JG and Topol EJ. Aortocoronary saphenous vein graft disease: pathogenesis, predisposition, and prevention. *Circulation*. 1998; 97: 916–31. [PubMed: 9521341]
18. Hoch JR, Stark VK, van Rooijen N, Kim JL, Nutt MP and Warner TF. Macrophage depletion alters vein graft intimal hyperplasia. *Surgery*. 1999; 126: 428–37. [PubMed: 10455917]
19. Mann MJ, Whittemore AD, Donaldson MC, et al. Ex-vivo gene therapy of human vascular bypass grafts with E2F decoy: the PREVENT single-centre, randomised, controlled trial. *Lancet*. 1999; 354: 1493–8. [PubMed: 10551494]
20. Jiang Z, Wu L, Miller BL, et al. A novel vein graft model: adaptation to differential flow environments. *AmJPhysiol Heart CircPhysiol*. 2004; 286: H240–H5.
21. Donadoni F, Pichardo-Almarza C, Bartlett M, Dardik A, Homer-Vanniasinkam S and Diaz-Zuccarini V. Patient-Specific, Multi-Scale Modeling of Neointimal Hyperplasia in Vein Grafts. *Front Physiol*. 2017; 8: 226. [PubMed: 28458640]
22. Mitsouras D, Owens CD, Conte MS, et al. In vivo Differentiation of Two Vessel Wall Layers in Lower Extremity Peripheral Vein Bypass Grafts: Application of High Resolution Inner-Volume Black Blood 3D FSE. *Magnetic resonance in medicine*. 2009; 62: 607–15. [PubMed: 19449380]
23. Mitsouras D, Mulkern RV, Owens CD, et al. High-resolution peripheral vein bypass graft wall studies using high sampling efficiency inner volume 3D FSE. *Magnetic resonance in medicine*. 2008; 59: 650–4. [PubMed: 18219632]
24. Mitsouras D, Mulkern RV and Rybicki FJ. Strategies for inner volume 3D fast spin echo magnetic resonance imaging using nonselective refocusing radio frequency pulses. *Med Phys*. 2006; 33: 173–86. [PubMed: 16485424]
25. Terry CM, Kim SE, Li L, et al. Longitudinal assessment of hyperplasia using magnetic resonance imaging without contrast in a porcine arteriovenous graft model. *Academic radiology*. 2009; 16: 96–107. [PubMed: 19064217]
26. Rybicki FJ, Mitsouras D, Owens CD, et al. Lower extremity peripheral vein bypass graft wall thickness changes demonstrated at 1 and 6 months after surgery with ultra-high spatial resolution black blood inner volume three-dimensional fast spin echo magnetic resonance imaging. *Int J Cardiovasc Imaging*. 2008; 24: 529–33.
27. Rybicki FJ, Mitsouras D, Owens CD, et al. Multi-contrast high spatial resolution black blood inner volume three-dimensional fast spin echo MR imaging in Peripheral Vein Bypass Grafts. *Int J Cardiovasc Imaging*. 2010; 26: 683–91. [PubMed: 20333469]
28. Mitsouras D, Vemula PK, Yu P, et al. Immobilized Contrast Enhanced (ICE) MRI: Gadolinium-based Long-term MR Contrast Enhancement of the Vein Graft Vessel Wall. *Magnetic resonance in medicine*. 2011; 65: 176–83. [PubMed: 20859994]
29. Nguyen B, Vemula P, Mitsouras D, et al. Immobilization of iron oxide magnetic nanoparticles for enhancement of vessel wall magnetic resonance imaging - an ex vivo feasibility study. *Bioconjug Chem*. 2010; 21: 1408–14012. [PubMed: 20608720]
30. Sarkar D, Vemula PK, Teo GS, et al. Chemical engineering of mesenchymal stem cells to induce a cell rolling response. *Bioconjug Chem*. 2008; 19: 2105–9. [PubMed: 18973352]
31. Yu P, Nguyen BT, Tao M, Bai Y and Ozaki CK. Mouse vein graft hemodynamic manipulations to enhance experimental utility. *The American journal of pathology*. 2011; 178: 2910–9. [PubMed: 21641408]
32. Yu P, Nguyen BT, Tao M, Campagna C and Ozaki CK. Rationale and practical techniques for mouse models of early vein graft adaptations. *Journal of vascular surgery*. 2010; 52: 444–52. [PubMed: 20573477]
33. Davies MG and Hagen PO. Pathophysiology of vein graft failure: a review. *European journal of vascular and endovascular surgery : the official journal of the European Society for Vascular Surgery*. 1995; 9: 7–18.
34. Crowe LA, Gatehouse P, Yang GZ, et al. Volume-selective 3D turbo spin echo imaging for vascular wall imaging and distensibility measurement. *J Magn Reson Imaging*. 2003; 17: 572–80. [PubMed: 12720267]
35. Luk-Pat GT, Gold GE, Olcott EW, Hu BS and Nishimura DG. High-resolution three-dimensional in vivo imaging of atherosclerotic plaque. *Magnetic resonance in medicine*. 1999; 42: 762–71. [PubMed: 10502766]

36. Gold GE, Han E, Stainsby J, Wright G, Brittain J and Beaulieu C. Musculoskeletal MRI at 3.0 T: relaxation times and image contrast. *AJR American journal of roentgenology*. 2004; 183: 343–51. [PubMed: 15269023]
37. Sadowski EA, Bennett LK, Chan MR, et al. Nephrogenic systemic fibrosis: risk factors and incidence estimation. *Radiology*. 2007; 243: 148–57. [PubMed: 17267695]
38. Soulez G, Bloomgarden DC, Rofsky NM, et al. Prospective Cohort Study of Nephrogenic Systemic Fibrosis in Patients With Stage 3–5 Chronic Kidney Disease Undergoing MRI With Injected Gadobenate Dimeglumine or Gadoteridol. *AJR Am J Roentgenol*. 2015; 205: 469–78. [PubMed: 26295633]

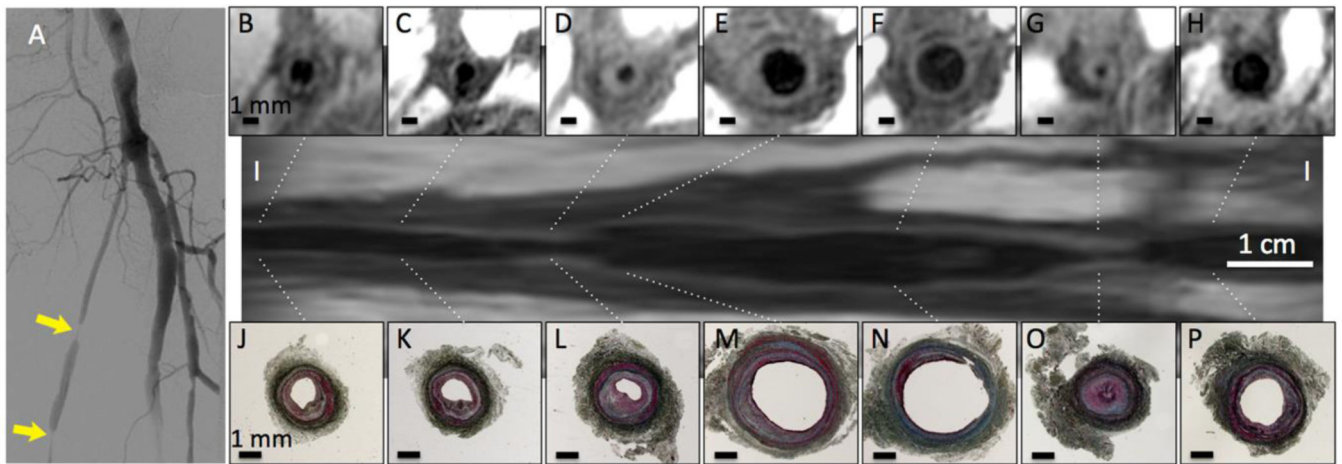


Figure 1.

In vivo T1W MRI of a failed 8-month-old human VG at a spatial resolution of 0.19 mm³ (2 mm slice thickness, 0.31 mm in-plane resolution) in 10 min scan time at 1.5 Tesla. MRI cross-sections (**B-H**) and curved multi-planar reformation (**I**) are in excellent agreement with corresponding Masson trichrome histology obtained after excision (**J-P**), for both intimal hyperplasia (all images) and wall remodeling (negative **B-D & G-H**; positive **E-F**). Conventional angiography (**A**) shows only lumen stenoses (arrows).

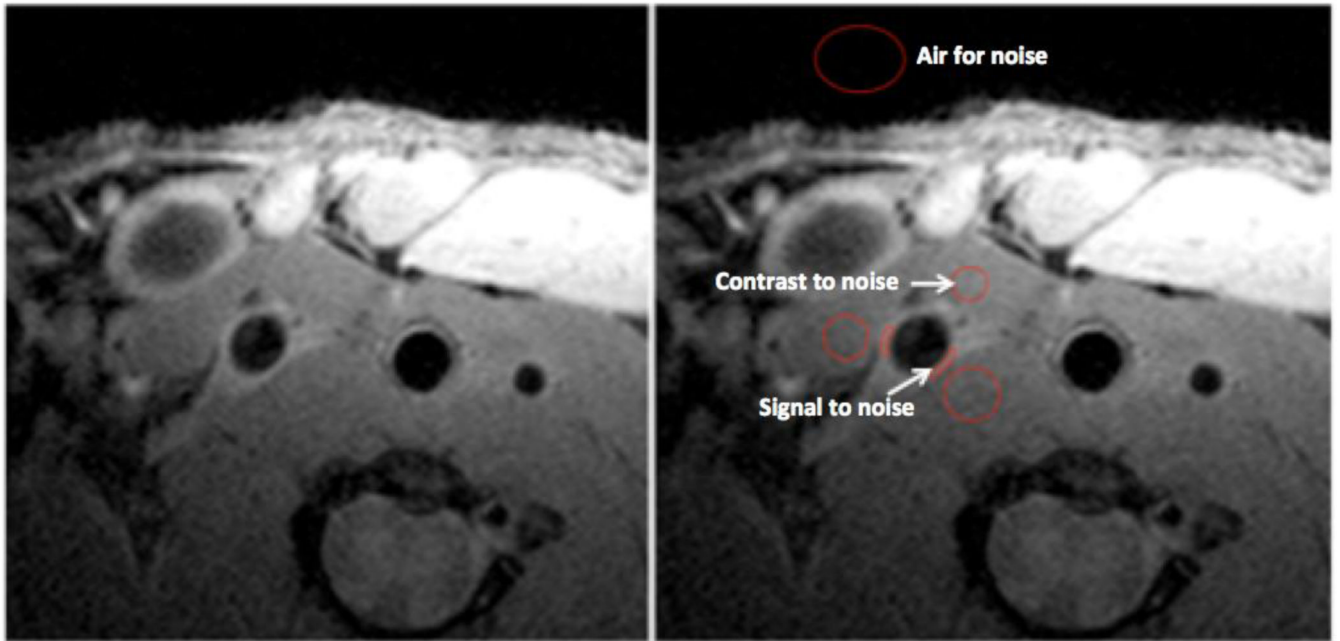


Figure 2.

In vivo 7 Tesla FLASH MRI of mouse interposition carotid vein graft at 4 weeks post-implantation. ROIs for MR signal measurements (air for noise, vein graft wall for signal-to-noise ratio and tissue surrounding vein graft for contrast-to-noise ratio) are shown in the right-hand panel.

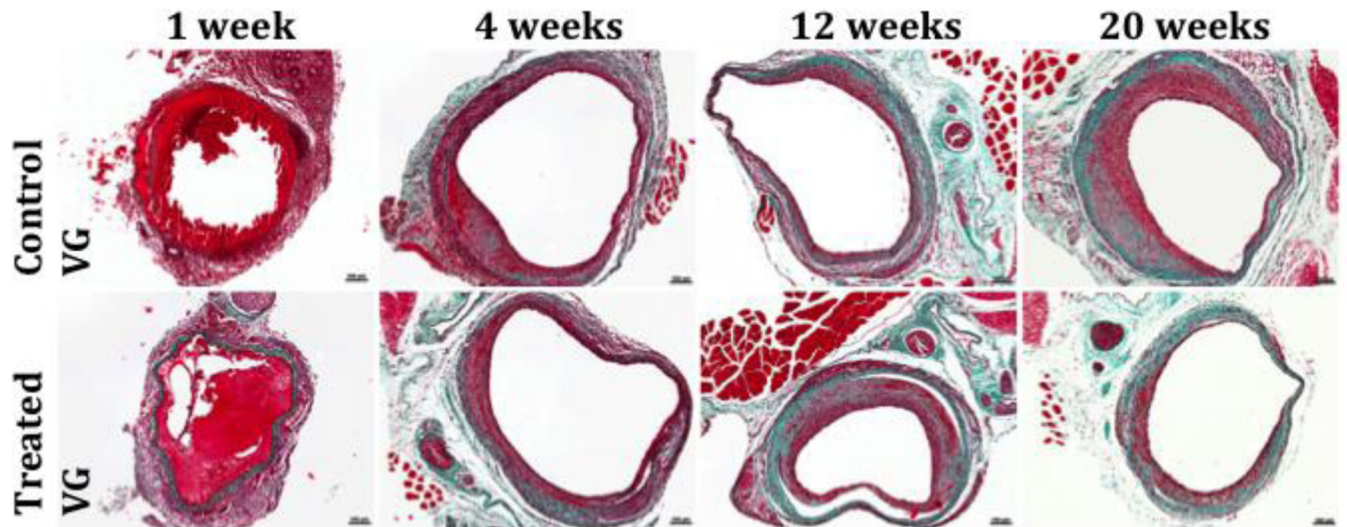


Figure 3.

Representative Masson's trichrome stained microscopic images of vein grafts in controls and treated mice. The specimens were collected and analyzed at 1, 4, 12, and 20 weeks postoperatively. The microscopic graphs were taken at 600 μm to the proximal cuff edges of the vein grafts. Scale bars = 100 μm .

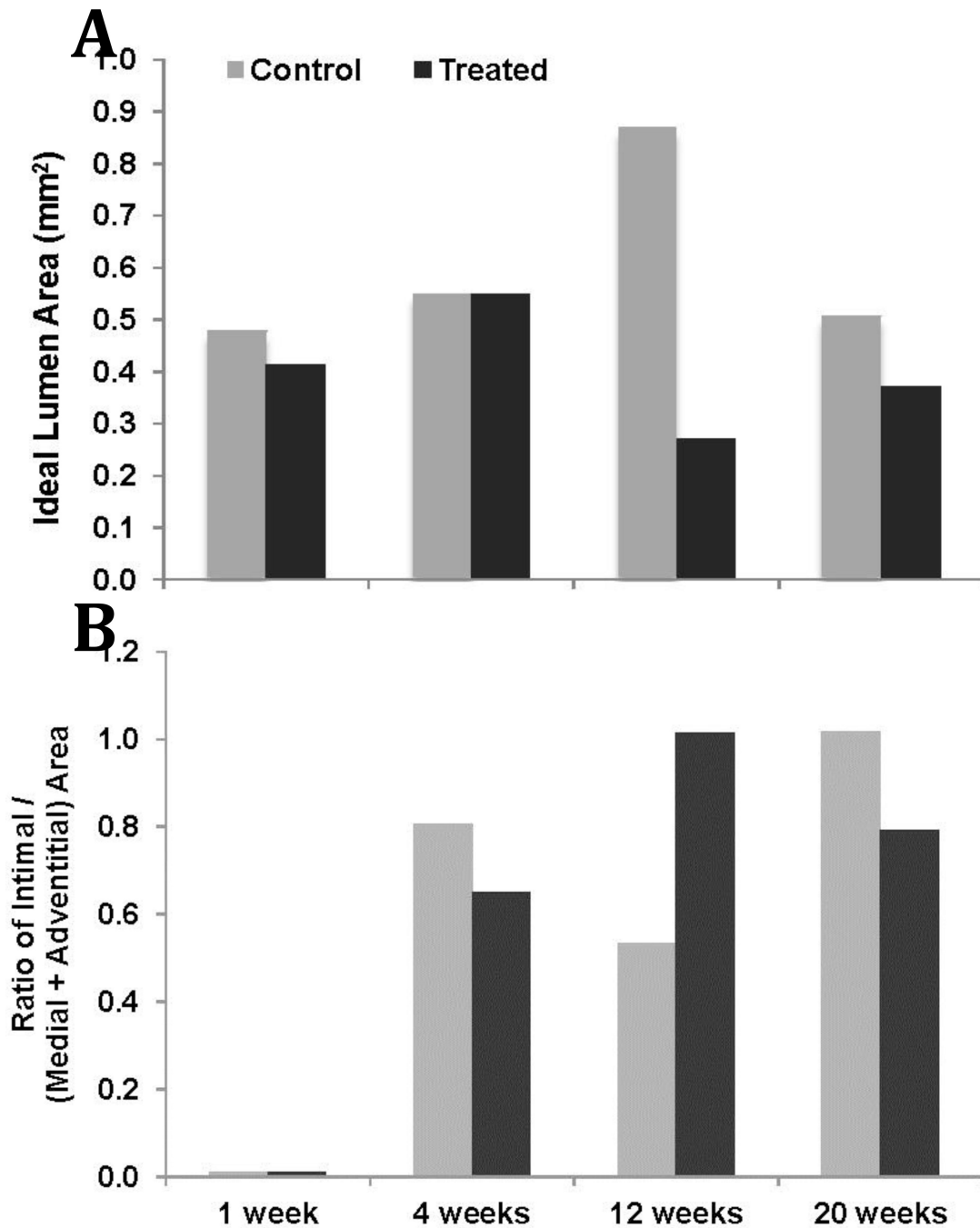


Figure 4.

Vein graft morphometric analysis at 1, 4, 12, and 20 weeks post the isograft carotid interposition vein grafts implantation; calculated Ideal luminal area in controls and treated mice (A), with each bar representing an average of at least 3 locations (200 μ m, 400 μ m, and 600 μ m) of vein grafts harvested at that time point ($n=1\sim 2$). Ratio of the intimal / (medial + adventitial) area in controls and treated vein grafts. Neointima development and (medial + adventitial) thickening were observed in both control and MRI contrast agent-treated vein grafts, with no apparent gross or microscopic differences observed between the two groups.

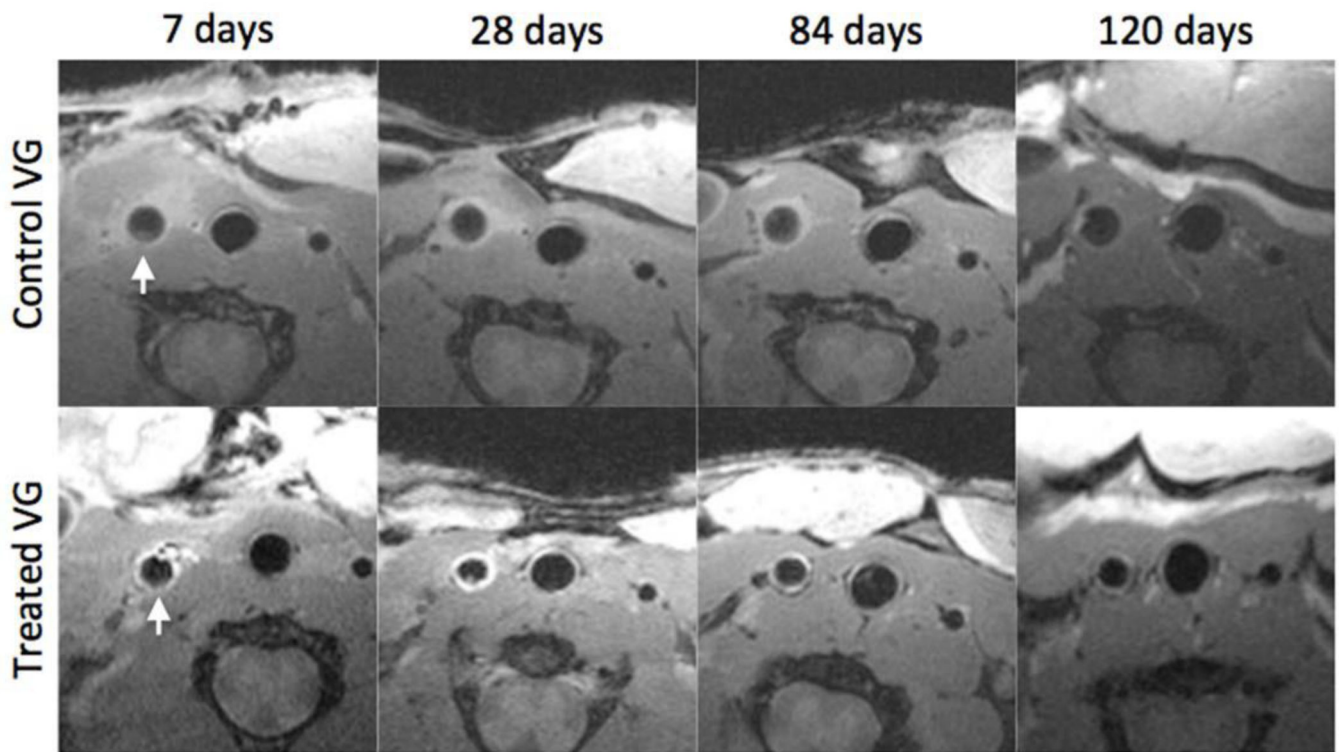


Figure 5. Longitudinal MRI of one control and one treated mouse included in study; in the control animal the vein graft (arrow) exhibits similar MRI signal at all 4 imaging time points (top row). The VG in the animal that received a Gd-DTPA labeled VG (arrow) shows increased signal and delineation from surrounding tissues at all time points (bottom row), although at 4 weeks enhancement is segmental (strongest at 12–3 and 4–6 o'clock) and further reduced at 20 weeks.

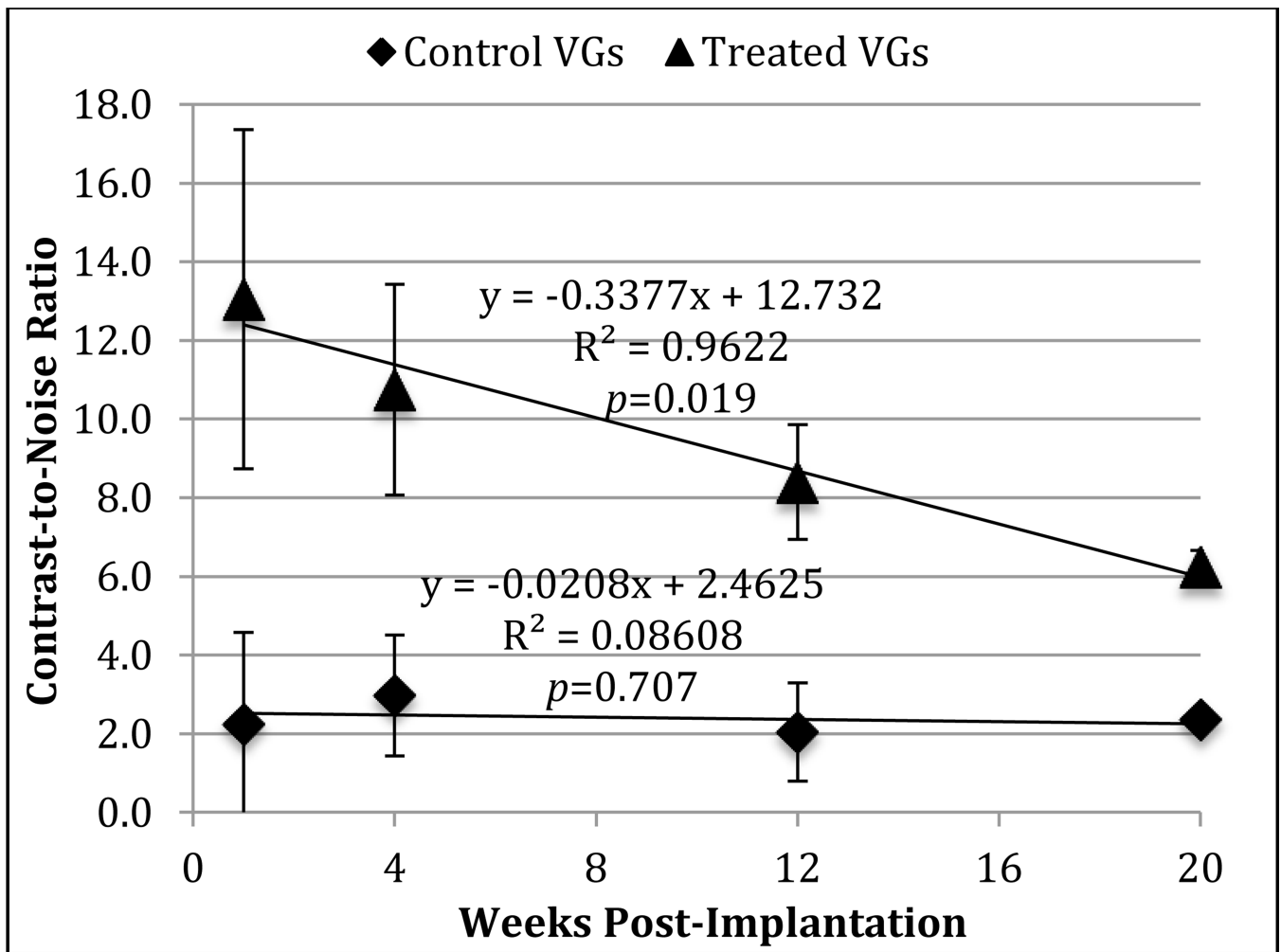


Figure 6. Average (\pm error bars) longitudinal CNR data from all 15 animals successfully imaged in the study (7 control, 8 labeled VG).

Control VGs maintained a stable CNR throughout the study period. The CNR of labeled VGs was higher than that of control VGs at all time points but decreased throughout the study period, as indicated by linear regression analyses.